

This is a postprint version of the following published document:

Ureña, J., Tejado, E., Pastor, J.Y., Velasco, F., Tsipas, S., Jiménez-Morales, A., Gordo, E. (2018). Role of beta-stabilizing elements on the microstructure and mechanical properties evolution of modified PM Ti surfaces designed for biomedical applications, *Powder Metallurgy*, 61(2), pp. 90-99.

DOI: 10.1080/00325899.2018.1426185

# Role of beta-stabilizing elements on the microstructure and mechanical properties evolution of modified PM Ti surfaces designed for biomedical applications

J. Ureña<sup>a</sup>, E. Tejado<sup>id b</sup>, J. Y. Pastor<sup>b</sup>, F. Velasco<sup>a,c</sup>, S. Tsipas<sup>id a,c</sup>, A. Jiménez-Morales<sup>a,c</sup> and E. Gordo<sup>id a,c</sup>

<sup>a</sup>University Carlos III of Madrid, Leganés, Spain; <sup>b</sup>Departamento de Ciencia de Materiales-CIME, Universidad Politécnica De Madrid, Madrid, Spain; <sup>c</sup>Alvaro Alonso Barba Technological Institute of Chemistry and Materials, IAAB, University Carlos III of Madrid, Leganés, Spain

## ABSTRACT

This work focuses on the evaluation of modified surfaces on Ti produced by powder metallurgy. These newly designed surface modifications are achieved by deposition and diffusion of a stable aqueous suspension prepared in one case from micro-sized Nb powder (Ti  $\beta$ -stabilizer element) and in another case from Nb plus the addition of ammonium chloride,  $\text{NH}_4\text{Cl}$ , (thermo-reactive diffusion process). Different design parameters such as diffusion element (Nb or Mo), state of the Ti substrate (green or sintered) and the treatment process (diffusion or thermo-reactive diffusion) lead to all the surface-modified materials, GreenTi-Nb, SintTi-Nb and Ti-Nb $_{\text{NH}_4\text{Cl}}$ , GreenTi-Mo, SintTi-Mo and Ti-Mo $_{\text{NH}_4\text{Cl}}$ . The modified Ti surfaces present a gradient in composition and microstructure ( $\beta$  /  $\alpha+\beta$  /  $\alpha$  phases) resulting in an improvement in some of their mechanical properties: (1) higher micro-hardness in all the modified materials and (2) lower elastic modulus (more similar to that of the human bone) in those without  $\text{NH}_4\text{Cl}$ .

## KEYWORDS

Titanium; surface-modification; powder technology; microstructural-gradient; elastic modulus; hardness

## 1. Introduction

The great interest of titanium alloys in the biomedical sector is well known due to their suitable characteristics for biomaterials compared to other metallic materials. However, there are still some concerns regarding titanium alloys such as the high Young's modulus which is superior to that of human bone, the low wear resistance and the toxic effect of Al and V of some alloys on the long term [1,2]. Among the desired properties of biomaterials, the mechanical ones are considered of high importance since an improvement in hardness together with a decrease in modulus of elasticity would enhance the service life period of implants [2, 3]. A large variety of properties can be achieved with titanium due to two main characteristics: (1) crystalline structure (hcp or bcc) with  $\alpha$ ,  $\alpha + \beta$  or  $\beta$  phase according to the  $\beta$ -transus temperature [4,5]; and (2) high susceptibility of being modified through surface modification treatments.

High specific strength is one of the main requirements for implants, and titanium has the most suitable value among the metallic biomaterials in this aspect [6]. However, the design of  $\beta$ -Ti alloys emerges as a response to the necessity of improving other poorer aspects such as stiffness.  $\beta$ -Ti alloys have low Young's modulus while maintaining or enhancing the material strength by incorporating biocompatible elements such as Mo, Nb, Zr or Ta which makes them ideal for biomedical applications [1,4,6]. Furthermore, Mo and

Nb exhibit complete solubility in Ti above 882°C which allows a microstructural change and thus, the modification of their properties [4,7]. However, a large amount of these alloying elements is required to maintain stable  $\beta$  phase at room temperature which raises the price and density of these alloys [8]. For this reason, the surface modification with  $\beta$ -stabilising elements is employed as a strategy to improve the surface properties while maintaining the lightness of Ti in the core.

Regarding surface modification, a wide variety of processes and techniques are employed for the enhancement of mechanical, biological and chemical properties of implants. Depending on the aspect to improve, the most widely used are: (i) *For wear resistance*, nitriding techniques such as diffusion, ion-plasma, laser, high-energy plasma methods for TiN synthesis [9,10] or laser cladding [11]; (ii) *for corrosion resistance*, physical and chemical vapour deposition [12], chemical/thermal treatment [13], thermal oxidation/spraying, plasma spray, ion implantation, micro-arc oxidation, sandblasting or electrochemical treatments; and (iii) *for mechanical performance and biocompatibility*, developing  $\beta$ -alloys by introduction of Nb, Zr, Mo, Ta or Sn [8], or physical or chemical treatments such as wet etching, anodisation or laser/plasma exposition [14,15]. A summary of these surface modifications has been reported in Refs. [16,17].

In this work, the diffusion of two different  $\beta$ -stabiliser elements, Nb or Mo, has been the approach followed toward enhancing the mechanical performance by reducing the modulus of elasticity and improving hardness. This approach modifies the surface properties of Ti, maintaining its lightness in the core. The modified Ti surfaces have been processed in two stages: (i) fabrication of Ti substrates by conventional powder metallurgy route of pressing and sintering, benefiting from the cost-effectiveness of this processes [18,19]; and (ii) a heat treatment to promote the diffusion of the deposited elements on the Ti substrates [5,8]. Therefore, the results of this paper are presented and discussed based on the influence of microstructure and chemical composition on the mechanical properties of different surface modifications performed as a function of diffusion element (Nb or Mo), state of the Ti substrate (green or sintered) and diffusion process (with or without activating agent).

## 2. Experimental procedure

### 2.1. Materials and sample preparation

The materials processed classified by their design parameters together with the nomenclature used further on are summarised in Table 1.

The surface modification carried out with niobium as diffusion element led to GreenTi-Nb, SintTi-Nb and Ti-Nb<sub>NH4Cl</sub> materials, whereas the molybdenum diffusion resulted in GreenTi-Mo, SintTi-Mo and Ti-Mo<sub>NH4Cl</sub> materials. All the six modified surfaces were studied and compared to Ti control as the reference material. First, the fabrication of the Ti substrates was carried out by using hydride-dehydride commercially pure titanium powder (cpTi grade 4) (GfE Metalle und Materialien GmbH, Germany) with a particle size below 75  $\mu\text{m}$ , and a mean particle size of 45  $\mu\text{m}$ . The green Ti substrates were produced by uniaxial pressing at 600 MPa using a cylindrical die of 16 mm in diameter with lubricated walls using zinc stearate. For the sintered Ti substrates, a sintering cycle in high vacuum ( $10^{-5}$  mbar) at 1250°C for 2 h

with a heating and cooling rate of  $5^\circ\text{C min}^{-1}$  was applied after pressing. Then, the surface modification by Nb was performed depositing an aqueous suspension of niobium powder with a particle size between 1 and 5  $\mu\text{m}$  (Alfa Aesar, Germany). A suspension containing 10% volume Nb particles was prepared in water and sprayed at room temperature onto the powder metallurgy (PM) Ti substrates in two different states: green Ti compact (as-pressed) and sintered Ti in order to obtain two different final materials. Before the niobium deposition, the surfaces of the sintered Ti substrates were prepared through grinding with 180# SiC paper and cleaning in an ethanol ultrasonic bath in order to remove any possible oxide formed. Then, the suspension was sprayed on green and sintered substrates. The Nb diffusion treatment was performed through a heat treatment in high vacuum ( $10^{-5}$  mbar) for 3 h at 1100°C and cooling at  $5^\circ\text{C min}^{-1}$ , obtaining the labelled GreenTi-Nb and SintTi-Nb materials. The same process was carefully followed to prepare the Mo suspension and obtain the GreenTi-Mo and SintTi-Mo materials as reported in a previous work [20]. Alternative to the high vacuum diffusion process, Ti-Nb<sub>NH4Cl</sub> and Ti-Mo<sub>NH4Cl</sub> materials were obtained through thermo-reactive diffusion in a controlled Ar atmosphere. An addition of 1.5% of NH<sub>4</sub>Cl (activating agent) was added to the niobium or molybdenum suspension to obtain the Ti-Nb<sub>NH4Cl</sub> and Ti-Mo<sub>NH4Cl</sub>, respectively. Both materials were subjected to a thermo-reactive diffusion process in Ar atmosphere at 1100°C with a dwell time of 3 h and a heating and cooling rate of  $5^\circ\text{C min}^{-1}$ . Finally, before each test, all the diffusion-treated surfaces were finished by a soft grind with a 1200# SiC emery paper followed by ultrasonic bath in propanol for 5 min.

### 2.2. Microstructural and chemical analysis

The cross-section of all the materials was examined to analyse microstructure and phase transformation by an FE-SEM (FEI Teneo) equipment. Chemical composition analysis was performed by an EDAX equipment in terms of profile and detailed mapping analysis. For this purpose, the cross-section of the materials was prepared by grinding with SiC emery paper from 180# to 1200# grade and polishing down to 0.3  $\mu\text{m}$  alumina suspension.

### 2.3. Mechanical testing: surface Vickers micro-hardness, surface macro-indentation and cross-sectional nanoindentation

Vickers micro-hardness was measured on the surfaces of the materials, applying a load of 100 g (HV<sub>0.1</sub>) for 10 s with a diamond tip in a Zwick Roell micro-hardness tester and processed by the ZH $\mu$  HD software.

**Table 1.** Surface-modified Ti materials studied with their design parameters.

| Materials              | Design parameters |    |                 |          |                   |      |
|------------------------|-------------------|----|-----------------|----------|-------------------|------|
|                        | Diffusion element |    | Substrate state |          | Treatment process |      |
|                        | Nb                | Mo | Green           | Sintered | Diffusion         | TRD* |
| Ti                     | —                 | —  | —               | —        | —                 | —    |
| GreenTi-Nb             | ■                 | —  | ■               | —        | ■                 | —    |
| SintTi-Nb              | ■                 | —  | —               | ■        | ■                 | —    |
| Ti-Nb <sub>NH4Cl</sub> | ■                 | —  | —               | ■        | —                 | ■    |
| GreenTi-Mo             | —                 | ■  | ■               | —        | ■                 | —    |
| SintTi-Mo              | —                 | ■  | —               | ■        | ■                 | —    |
| Ti-Mo <sub>NH4Cl</sub> | —                 | ■  | —               | ■        | —                 | ■    |

\*TRD: Thermo-reactive diffusion (with the activating agent (NH<sub>4</sub>Cl)).

Six measurements were performed on each material in order to get a reliable average.

Macroscale surface indentation measurements were performed, and Vickers hardness, elastic modulus and maximum indentation depths were determined applying a load of 5 N with a speed for load application of  $0.5 \text{ mm min}^{-1}$  and a speed for load removal of  $2 \text{ mm min}^{-1}$  in a Zwick Roell Z 2.5 tester. The effect of load was studied applying a bigger load of 15 N. Mean E and H values of all the materials were expressed as the average of six different measurements.

Nanoindentation measurements in the cross-section were performed to obtain a more precise response and evaluate the effect of microstructure and chemical composition on hardness and elastic modulus. They were carried out to a depth of 500–750 nm with 10 mN as maximum load by using a standard Berkovich tip calibrated by fused silica. The measurements were performed in an MTS Nanoindenter equipment in profiles from the outer area to the inner part. The average values were calculated by three measurements at different points of the diffusion layers and substrate areas.

### 3. Results and discussion

#### 3.1. Microstructure and chemical characterisation

Figure 1 shows the microstructure of the three modified Ti–Nb surfaces. A gradient of microstructure and composition was observed in Figure 1(a and b) with diffusion areas of 100–120  $\mu\text{m}$  depth depending on the initial state of the Ti substrate. Nb diffusion changed the microstructure of  $\alpha$ -single-phase titanium into a gradient of  $\beta \rightarrow \alpha + \beta \rightarrow \alpha$  phases moving inward. Moving towards the external surface, the  $\alpha + \beta$  lamellae appeared closer together, becoming a single

$\beta$  region rich in Nb (detailed in-view from Figure 1(a)). In the case of the surface modification in green substrate (GreenTi–Nb), the diffusion area of 120  $\mu\text{m}$  confirms the successful surface modification in a single step during a co-sintering process. On the other hand, Figure 1(b) shows the surface modification carried out in sintered Ti substrate (SintTi–Nb) which is homogeneous and reaches about 100  $\mu\text{m}$  depth. Both micrographs present brighter zones in the upper part corresponding with the rests of non-diffused niobium particles which remain adhered to titanium. An energy dispersive X-ray (EDS) profile was taken from Figure 1 (b) to observe the distribution of the elements along the depth. From this analysis, it can be stated that the first 10  $\mu\text{m}$ , approximately, correspond to the total diffusion of Nb in the Ti matrix due to its high solubility into titanium according to the Ti–Nb phase diagram [7]. Moving inwards, the niobium content starts to decrease while the amount of titanium increases, and the  $\alpha$ – $\beta$  phase appears in the microstructure. The niobium content in the Nb-rich region was of 90%, decreasing until 50% at a depth of 10  $\mu\text{m}$  and varying between 30% and 10% as the beta lamellae become more separated. Similar Ti–Nb diffusion profiles simulated at the same temperature as ours have been reported in the recent literature [4]. The peaks observed in the composition profile correspond to the separated  $\beta$  lamellae, becoming almost zero at the depth of 100  $\mu\text{m}$ . However, a different structure was found for the Ti–Nb<sub>NH<sub>4</sub>Cl</sub> material (Figure 1(c)) created by a thermo-reactive diffusion process with the addition of an activating agent to stimulate the diffusion phenomena due to the formation of volatile Nb chlorides. This method has been already used in other investigations with the aim of increasing surface hardness and creating diffusion layers [13,21]. Owing to the addition of the ammonium chloride activator, titanium nitride is created on the surface, leading to

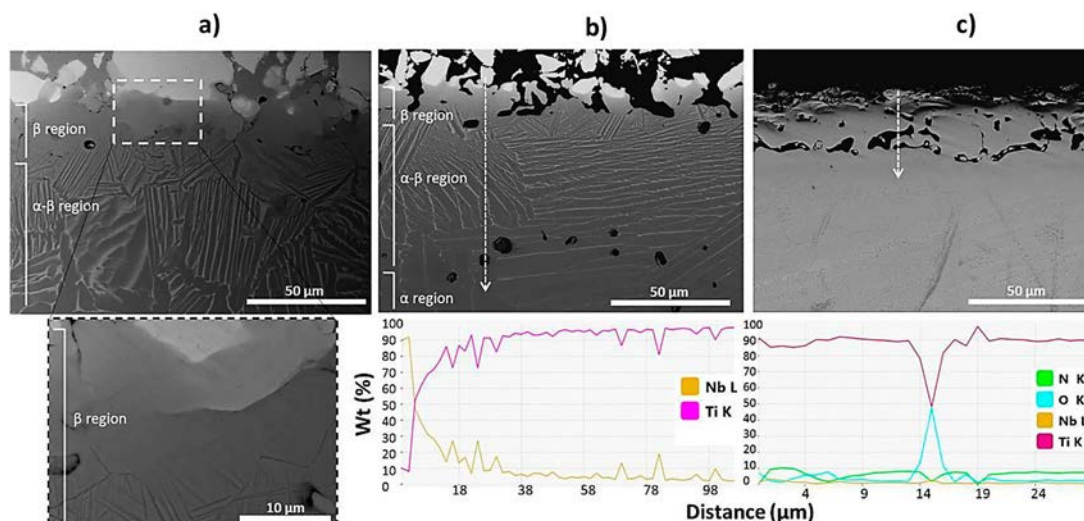


**Figure 1.** BSE SEM micrographs of the cross-section for the modified PM Ti surfaces with niobium: (a) GreenTi–Nb, (b) SintTi–Nb and (c) Ti–Nb<sub>NH<sub>4</sub>Cl</sub>. Diffusion areas and EDS profiles.

some nitrogen diffusion inwards which can improve the material surface hardness. The  $\alpha + \beta$  regions were not identified in that case, and Nb remained on the surface in very low percentage. Some porosity typical from the thermo-reactive diffusion process appeared in the upper part [21]. As expected, the EDS profile indicated some nitrogen diffusion of almost 10%, constant in the first micrometres. The strong oxygen peak corresponds to a pore since the chemical analysis was performed crossing the porous area. This porosity may be an interesting result from a biomedical point of view to improve cell attachment and proliferation [22].

Besides Nb diffusion,  $\beta$ -phase formation from  $\alpha$ -structure has been achieved by molybdenum diffusion (Figure 2). Molybdenum diffusion seemed to act in the same way as niobium: creating the  $\beta \rightarrow \alpha + \beta \rightarrow \alpha$  microstructural gradient together with a Ti–Mo compositional gradient (Figure 2(b)). The surface modification was also performed on green and sintered Ti substrates (Figure 2(a and b)), respectively. A detailed view of the  $\beta$ -region is shown in Figure 2(a). From the EDS profile analysis (Figure 2(b)), it was possible to observe that the upper part corresponds to a 10- $\mu\text{m}$  Mo-rich region of approximately 60% Mo diffused in and 40% Ti. The Mo content decreases from surface inwards up to 90  $\mu\text{m}$  depth. As a result, a diffusion layer of similar characteristics was obtained for the SintTi–Mo and for the SintTi–Nb materials. Similar results were expected due to the analogous properties for both elements (Mo and Nb) and very similar phase diagrams. However, niobium seems to reach a slightly higher diffusion depth than molybdenum as well as an external part richer in niobium (90%) than in molybdenum (60%). This can be ascribed to higher diffusion coefficients for Ti–Nb systems as stated in Refs. [4,23]. On the other hand, the thermo-reactive diffusion process originated the porous Ti–Mo<sub>NH4Cl</sub>

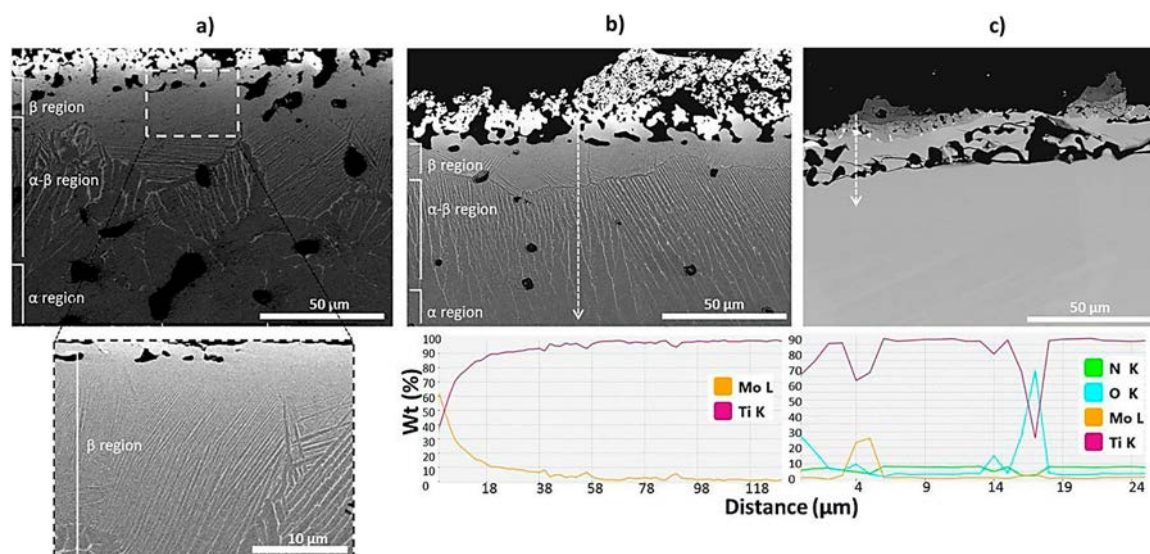
where the EDS graph shows a small diffusion of molybdenum and oxygen in the first micrometres and the nitrogen content remaining almost constant between 5% and 10%. This TiN surface (Figure 2(c)) can be compared to similar results reported in Ref. [21], showing an agreement between the porosity created by the activator and the absence of beta lamellae due to the nitrogen diffusion.

Figure 3 shows the element distribution (Figure 3 (a)) and a detailed view of the beta lamellae (Figure 3 (b)) formed on SintTi–Nb materials. In Figure 3(a), it can be seen how the  $\alpha + \beta$  region appears within the first 8- $\mu\text{m}$  region due to the fact that the  $\beta$ -stabiliser content is not enough to retain the  $\beta$ -phase. Figure 3 (b) presents a detailed micrograph of the  $\alpha + \beta$  region together with an EDS mapping. As a result of Nb diffusion, the  $\beta$  lamellae were randomly formed with broader and thinner zones becoming more dispersed in the bottom area due to the decreasing Nb content. Regarding the phase quantification for a determined area of the  $\alpha + \beta$  region, 17% of  $\beta$ -phase was found whereas the rest corresponds to the  $\alpha$ -phase.

### 3.2. Mechanical properties:

#### 3.2.1. Surface Vickers micro-hardness ( $HV_{0.1}$ )

Surface micro-hardness results on the modified surfaces are shown in Figure 4. Higher values were found with respect to bare Ti in the range of 2.9–3.1 GPa for the Ti–Nb surfaces and 3.6–4.2 GPa for the Ti–Mo. These values are comparable to those obtained in other related studies with similar Mo [24] or Nb contents [25], although slightly higher values were reported for Ti–Nb compositions with higher sintering temperature [7]. However, when comparing the co-sintered and the diffusion-treated samples, considerably higher differences were observed on the



**Figure 2.** BSE SEM micrographs of the cross-section for the modified PM Ti surfaces with molybdenum: (a) GreenTi–Mo, (b) SintTi–Mo and (c) Ti–Mo<sub>NH4Cl</sub>. Diffusion areas and EDS profiles.

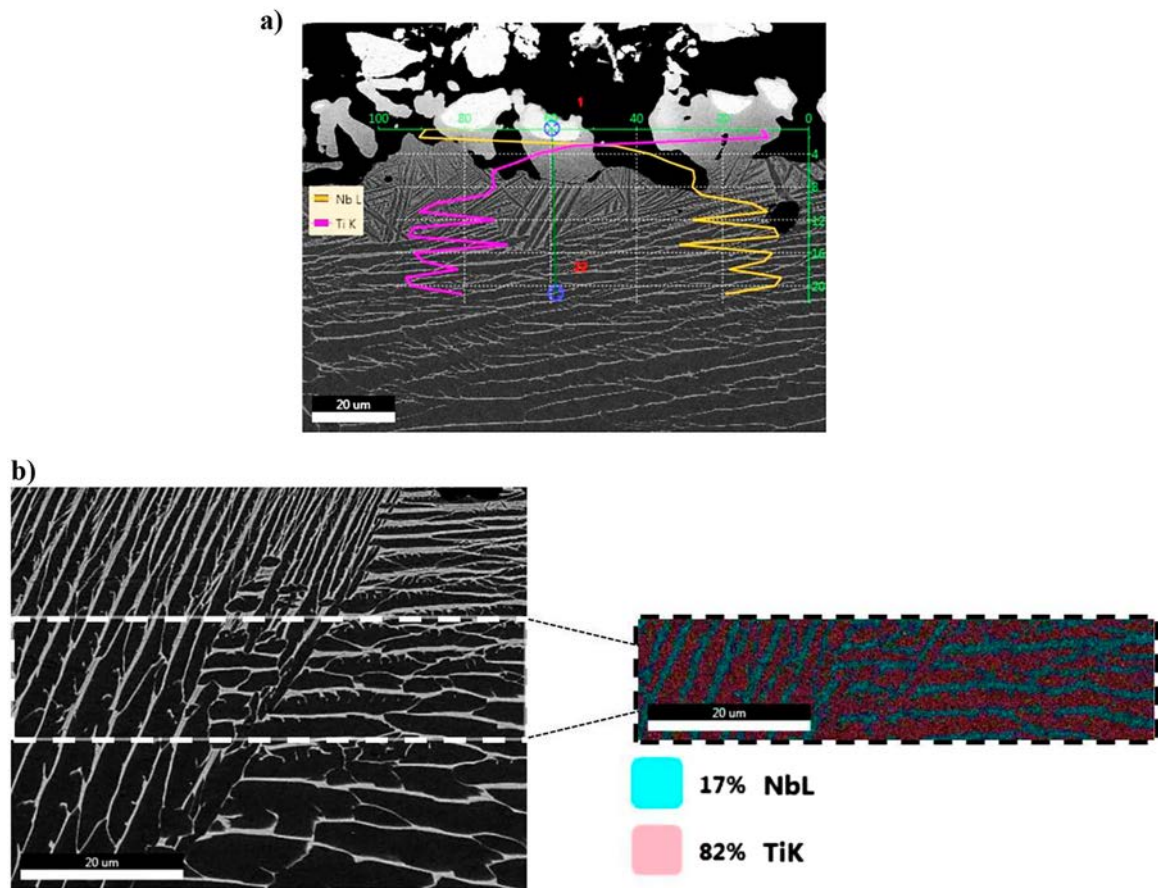


**Figure 3.** (a) Profile line analysis and (b) phase mapping showing the element distribution and phase transformation for the SintTi-Nb material.

Ti-Mo materials. This can be ascribed to the porosity and homogeneity of microstructures shown in Figures 1 and 2, where both of Ti-Nb surfaces exhibit similar diffusion layers, whereas GreenTi-Mo presents higher porosity than SintTi-Mo.

Another interesting issue is the higher average hardness noticed clearly on the modified Ti samples with Nb/Mo and the addition of the activator. As expected, the TiN created on these surfaces together with some nitrogen diffusion lead to an increase in hardness near to 8.6 and 10.1 GPa, respectively, which means more than three times the hardness of titanium. The difference between Nb and Mo may be related to the higher hardenability of Mo probably due to a higher solid solution strengthening effect [14]. In this context, it appears that Nb diffusion is slightly higher than Mo and thus, the formation of a higher amount of softer  $\beta$ -phase can be affecting the hardening effect. The increased average surface micro-hardness of the samples agrees with diffusion studies employing this technique to improve wear resistance and oxidation behaviour [26,27].

### 3.2.2. 5 N and 15 N indentation: surface elastic modulus and macro-hardness

In order to evaluate the hardness response of these materials at the macroscale, load-unload curves at

5 N and 15 N load were performed. From them, hardness and elastic modulus were obtained and represented in Figure 5. Regarding hardness, similar average values for both loads without significant difference were found. Nevertheless, the hardest surfaces (Ti-Mo<sub>NH4Cl</sub> and Ti-Nb<sub>NH4Cl</sub>) showed higher susceptibility to load since a decrease of around one order of magnitude was observed. This could be ascribed to their diffusion areas (Figures 1(c) and 2(c)) with the high porosity along the first 20–30 micrometres. Porosity is considered as one of the most relevant aspects that could affect hardness. Therefore, it can be noticed that the halide activator leads to a high increase in hardness as well as a higher susceptibility to load. Comparing micro-hardness (HV<sub>0.1</sub>) and macro-hardness (15 N) tests, slightly smaller values with bigger load can be observed. This is known as indentation size effect which means higher hardness with low loads [28].

Regarding stiffness, a decrease in elastic modulus is reached on the  $\beta$ -Ti surfaces as a result of the surface modification by  $\beta$ -stabilising element diffusion. The elastic modulus values obtained for both Ti-Nb and Ti-Mo were around 95 GPa, reaching a value of 80 GPa in the case of the co-sintered surface as a consequence of higher porosity. Similar values are reported for some metallic biomaterials such as 93, 78 and 75 GPa for Ti-10Mo, Ti-15Mo and Ti-20Mo,

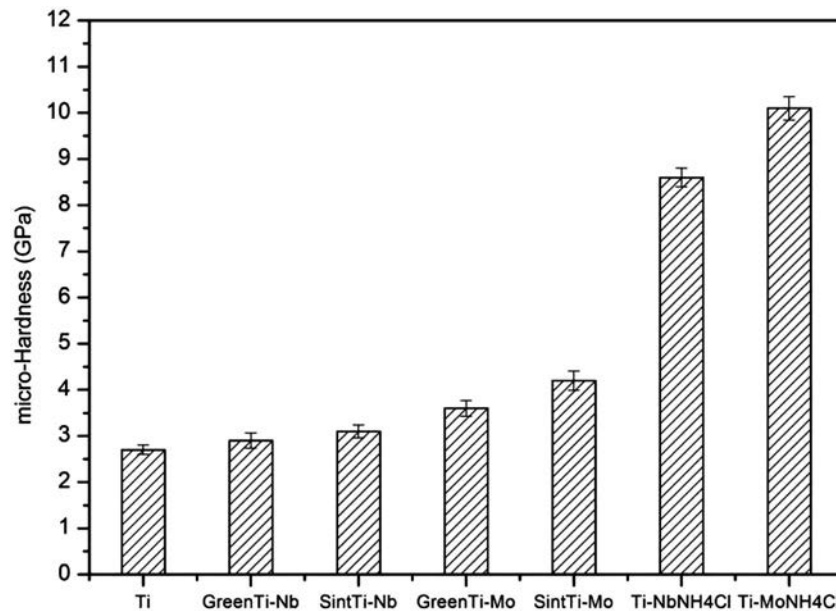


**Figure 4.** Vickers micro-hardness ( $HV_{0.1}$ ) tests for all the modified materials. The data are presented in GPa showing the mean value of the measurements and the standard deviation with vertical bars.

respectively [29,30]. However, the activated samples exhibited higher elastic modulus around 125–140 GPa mainly attributed to the TiN layer.

Figure 6 shows the diffusion layers depth together with the maximum indentation depth at 5 N and 15 N. In all samples, the maximum indentation depth did not exceed the diffusion areas, reaching values close to 20  $\mu\text{m}$  for the samples with lower stiffness which corresponds to the upper part ( $\beta$ -region). When comparing GreenTi–Nb and SintTi–Nb samples, higher porosity in the co-sintered samples seems to lead to a small increase of the indentation depth.

In this context, the surface porosity on the activated samples could suggest deeper indentation marks.

Nevertheless, these samples present the smallest values mainly attributed to their higher hardness. Therefore, it could be stated that hardness has a stronger influence on the maximum depth indentation than porosity, with hardness improvement resulting in smaller indentation depth with respect to Ti.

### 3.2.3. Nanoindentation: cross-sectional elastic modulus and nano-hardness

Hardness and elastic modulus values from nanoindentation measurements on the materials cross-section are summarised in Figure 7. A decrease in the average elastic modulus value on the diffusion layers (60–75 GPa) with respect to the substrate area was observed for all materials, except for the activated Ti–MoNH<sub>4</sub>Cl. As

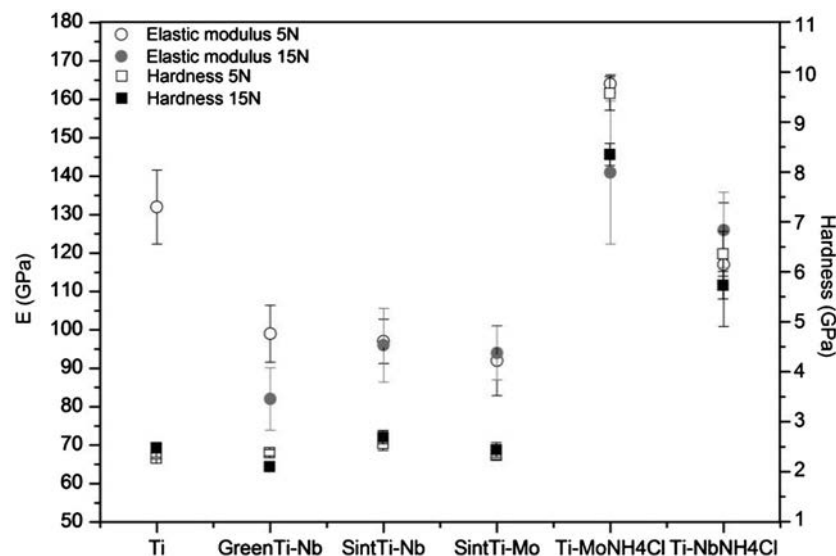


**Figure 5.** Elastic modulus and hardness values obtained from 5 N and 15 N indentation tests. The graph shows the mean value of the measurements and the standard deviation with vertical bars.

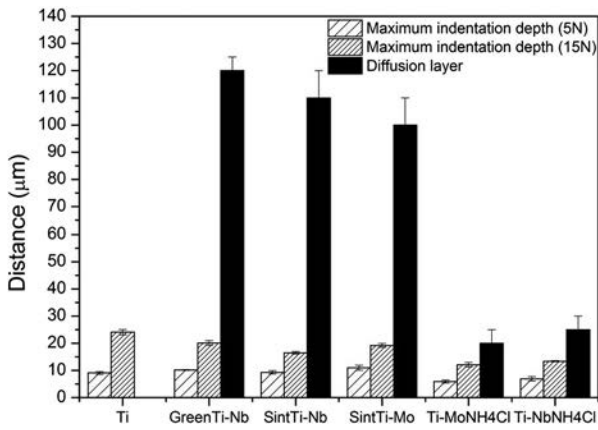


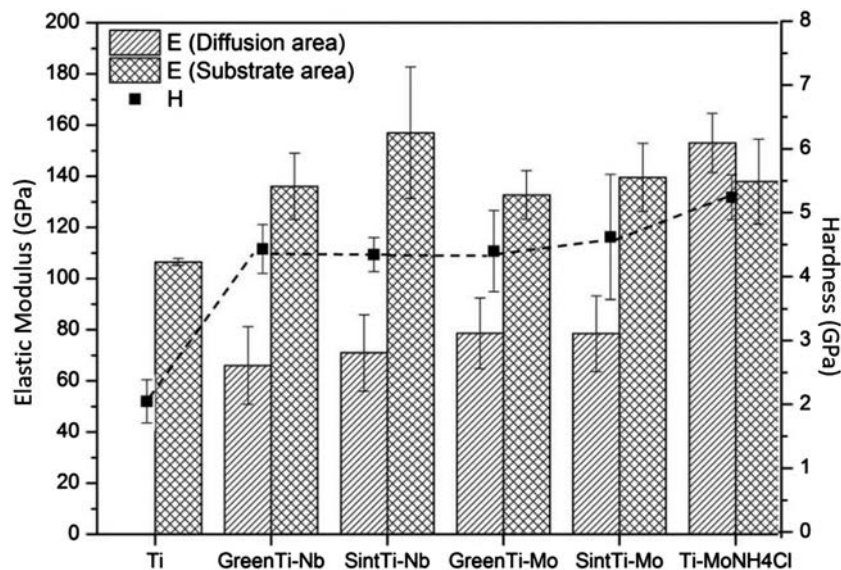
**Figure 6.** Comparison of the maximum indentation depth between 5 N and 15 N load for all the modified materials. The graph presents the mean value of the measurements and the standard deviation with vertical bars.

expected, the  $\beta$ -stabilising elements reduced the elastic modulus because of the  $\beta$ -phase formation, while the TiN layer from the Ti-Mo<sub>NH4Cl</sub> surface leads to increase in hardness but also elastic modulus. Furthermore, the elastic modulus seems to be slightly influenced by the initial state of the Ti substrate, with the GreenTi-Nb material presenting around 5 GPa less with respect to SintTi-Nb. Similar results are reported in the literature, with the  $\alpha$ -phase transformation into  $\beta$  or  $\alpha + \beta$  phases influenced by composition (i.e. Ti<sub>x</sub>Mo, Ti<sub>x</sub>Mo<sub>y</sub>Nb) [31,32]. Regarding hardness, values were higher in all the modified Ti materials around 4.5 GPa in agreement to that reported for a PM Ti-Nb alloy [7]. This means twice the hardness of bare Ti and near three times in the case of Ti-Mo<sub>NH4Cl</sub>.

Figure 8 shows the evolution of elastic modulus along depth where values corresponding to the

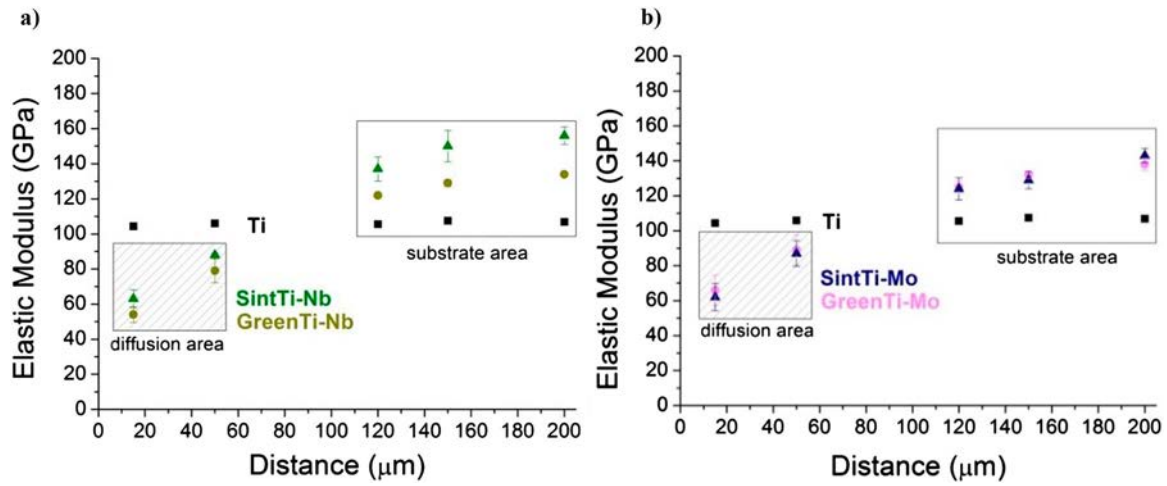
diffusion layers are shown in striped areas while those from the substrate area in empty squares. As it can be seen, similar features were obtained on both Ti-Nb and Ti-Mo systems, Figure 8(a) and (b), respectively. As a result of gradient microstructures and compositions, a gradient in elastic modulus was found on all the modified materials. The lowest values around 60 GPa were found closer to the surface (15  $\mu$ m depth), whereas medium values around 80 GPa at 50  $\mu$ m depth and above 110 GPa in the substrate area. These values are related to the microstructure of the materials, since the lowest E values were found in the outer part which means in the  $\beta$  region, the medium E values getting deeper into the  $\alpha + \beta$  region, and the highest E values in the  $\alpha$  region of the substrate area. However, E values corresponding to the  $\alpha$ -phase were slightly higher with respect to Ti whose microstructure is composed of  $\alpha$ -single phase. This could be ascribed to the heat treatment performed to promote the diffusion after the sintering cycle which means two heat treatments compared with only the sintering treatment of titanium. This could be attributed to reduced porosity and thus increased elastic modulus in those regions without  $\beta$ -stabilising element. This also agrees to the fact that the E values from the substrate area on the modified green samples are lower than their respective modified sintered samples.

Figure 9 shows the evolution of elastic modulus with the Nb and Mo composition (Figure 9(a) and (b)), respectively. Regarding Nb composition (Figure 9(a)), the lowest E value reached was 54 GPa with 20% of Nb on GreenTi-Nb material, while a slight increase up to 64 GPa was obtained with a higher amount of Nb (30%) on SintTi-Nb. This behaviour could be attributed to the relative higher porosity remaining in



**Figure 7.** Comparison of the average values of the elastic modulus between diffusion and substrate areas. Mean hardness of each material. Data obtained from nano-indentation test. The graph shows the mean value of the measurements and the standard deviation with vertical bars.





**Figure 8.** Evolution of elastic modulus as a function of distance on (a) Ti–Nb and (b) Ti–Mo systems. The graphs show the mean value of the measurements and the standard deviation with vertical bars.

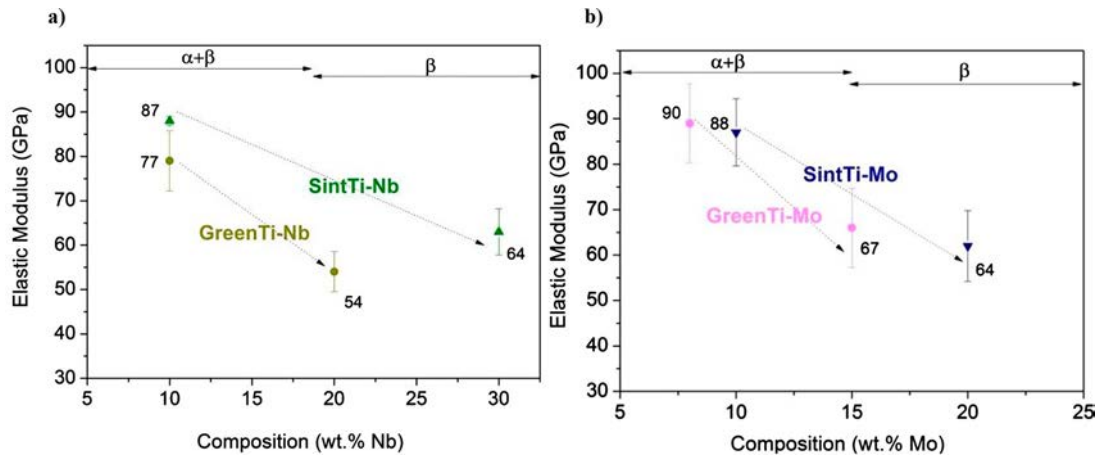


**Figure 9.** Evolution of elastic modulus as a function of (a) Nb and (b) Mo composition. The graphs show the mean value of the measurements and the standard deviation with vertical bars.

the Green material due to its fabrication route in only one single step. These E values correspond to the Nb-rich region composed of stable  $\beta$ -phase as reported in the Ti–Nb phase diagram [4]. When the Nb content decreased to 10% ( $\alpha + \beta$  region), E values raised up to 77 and 87 GPa, keeping the tendency of lower and higher elastic modulus on green and sintered samples, respectively. Similar values to those of our  $\beta$ -Ti surfaces around 60–70 GPa were reported for  $\beta$ -Ti alloys composed of two  $\beta$ -stabilising elements in different compositions such as Ti<sub>15</sub>Zr<sub>10</sub>Nb, Ti<sub>27</sub>Nb<sub>13</sub>Zr or Ti<sub>30</sub>Cr<sub>10</sub>Nb [31,33,34].

The elastic modulus as a function of Mo composition is shown in Figure 9(b). The lowest E value reached was 63 GPa on the SintTi–Mo sample with 20% of Mo. Whereas on GreenTi–Mo, as in the case of Nb, a low value of 65 GPa with only 15% of Mo was reached due to the slightly higher porosity. Similar to Figure 9(a), the microstructural change to  $\alpha + \beta$  resulted in E values close to 90 GPa with approximately 10% of Mo. Similar behaviour was reported for Ti–Mo

alloys exhibiting 13% of Mo and 75 GPa elastic modulus [14]. When comparing the  $\beta$ -stabiliser effect of Nb or Mo on Ti, relative lower elastic modulus values were reached by Nb diffusion with respect to those achieved by Mo diffusion. A good *in vitro* biological response has been reported for Ti–Mo–Nb with different compositions and E values around 80 GPa [32]. Therefore, this improvement in mechanical properties could lead to a promising biological response of our modified Ti surfaces.

#### 4. Conclusions

The surface modification by Nb and Mo diffusion treatments into Ti substrates processed by powder metallurgy has been successfully achieved. Three different Ti–Nb surfaces as well as three Ti–Mo surfaces have been designed. For the co-sintering and diffusion processes, well-defined gradients in microstructure ( $\beta / \alpha + \beta / \alpha$ ) and composition (Ti–Nb or Ti–Mo) with Nb-rich or Mo-rich surfaces were

obtained. These diffusion layers ranged from 90 to 120  $\mu\text{m}$  in depth while thermo-reactive diffusion led to 20–25  $\mu\text{m}$  porous surfaces with a TiN layer on surface.

Hardness and elastic modulus were measured at different scales: (i) surface Vickers micro-hardness ( $\text{HV}_{0.1}$ ), (ii) 5 N and 15 N surface macro-indentation and (iii) cross-sectional nanoindentation. The micro-structural gradient on the materials resulted in a gradient in mechanical properties as well as lower elastic modulus values at the Nb-rich or Mo-rich regions composed of fully  $\beta$ -phase: 54 GPa (GreenTi–Nb), 64 GPa (SintTi–Nb), 65 GPa (GreenTi–Mo) and 63 GPa (SintTi–Mo). A decrease up to 40–50% with respect to the elastic modulus of two of the most used Ti alloys for biomedical applications: Cp-Ti (102–105 GPa) and Ti6Al4V (110–114 GPa) was achieved. The hardness of the modified surfaces was around 4 GPa, twice the value of pure Ti. The activated material exhibited the hardest surface, while a decrease in elastic modulus was not reached due to the lack of Mo diffusion and remanence of the  $\alpha$ -phase. Therefore, the improved hardness and decreased elastic modulus of these modified Ti surfaces enhanced the mechanical properties of Ti making them potentially suitable for biomedical applications.

## Disclosure statement

No potential conflict of interest was reported by the authors.

## Funding

The authors would like to thank the funding provided for this research by the Regional Government of Madrid (program MULTIMAT-CHALLENGE-CM, ref. S2013/MIT-2862), and by the Ministry of Economy and Competitiveness of Spain (program MINECO, ref. PCIN-2016-123 and Ramón y Cajal contract RYC-2014-15014).

## Notes on contributors

**J. Ureña** was born on November 26th, 1990 in Jaén/Spain. She studied chemistry at the University of Jaén from 2008 to 2012. Now, she is working in her PhD in material engineering from 2014 at the Group of Powder Metallurgy (GTP) of the University Carlos III of Madrid.

**E. Tejado** was born on September 24th, 1985 in Cáceres/Spain. She studied Building and Materials Engineering at the University of Extremadura. In 2017 she finished her PhD at the Materials Science Department of the Technical University of Madrid where she is actually working as an Assistant Professor.

**J. Y. Pastor** was born on October 26th, 1965 in Madrid/Spain. He studied physics and physics of materials in the Complutense University of Madrid from 1983 to 1988. In 1993, he finished his PhD in the Complutense University of Madrid. Now, he is Full Professor of Material Science and Engineering and Director of the Materials for the Future

Cluster of the International Campus of Excellence-Moncloa in the Technical University of Madrid.




**F. Velasco** has a PhD in Materials Science and Metallurgical Engineering in 1995 at University Politecnica of Madrid, Spain. He is professor at University Carlos III of Madrid since 1997. He has carried out research in sintered materials, corrosion and oxidation processes, adhesives, surface treatments and organic coatings.

**S. Tsipas** received her MEng degree in Materials Science and Engineering from Imperial College, London, United Kingdom in 2000 and completed her PhD in 2006 at the Department of Materials Science and Metallurgy in the University of Cambridge, United Kingdom. She was a post-doctoral researcher at the University Complutense of Madrid, Spain in 2006–2008. Since 2008 she works at University Carlos III of Madrid, Spain.

**A. Jiménez-Morales** is PhD in Industrial Technology (1999) from University Carlos III of Madrid, Spain. She is member of the Powder Metallurgy Group of the University Carlos III of Madrid. She has received the Award of Excellence in 2015 by the Social Council of the UC3M, the Santander Bank and Airbus. Her research is mainly focused on coatings and surface treatments, and powder injection molding processing.

**E. Gordo** is PhD in Mining Engineering (1998) from Technical University of Madrid, Spain. She obtained recently a full professor position at the University Carlos III of Madrid, Spain, where she was associated professor from 2003. Her research is mainly focused in the design and processing of titanium alloys and hardmetals by powder metallurgy.

## ORCID

**E. Tejado**  <http://orcid.org/0000-0002-5240-6702>  
**S. Tsipas**  <http://orcid.org/0000-0001-7590-2795>  
**E. Gordo**  <http://orcid.org/0000-0002-2869-1363>

## References

- [1] Niinomi M. Mechanical biocompatibilities of titanium alloys for biomedical applications. *J Mech Behav Biomed Mater.* 2008;1(1):30–42.
- [2] Hussein M, Mohammed A, Al-Aqeeli N. Wear characteristics of metallic biomaterials: a review. *Materials (Basel).* 2015;8(5):2749–2768.
- [3] Geetha M, Singh AK, Asokamani R, et al. Ti based biomaterials, the ultimate choice for orthopaedic implants – a review. *Prog Mater Sci.* 2009;54(3):397–425.
- [4] Zhu L, Zhang Q, Chen Z, et al. Measurement of inter-diffusion and impurity diffusion coefficients in the bcc phase of the Ti–X (X = Cr, Hf, Mo, Nb, V, Zr) binary systems using diffusion multiples. *J Mater Sci.* 2017;52(6):3255–3268.
- [5] Liu X, Chu PK, Ding C. Surface modification of titanium, titanium alloys, and related materials for biomedical applications. *Mater Sci Eng R Reports.* 2004;47(3–4):49–121.
- [6] Goraiinov V, Cook R, Latham JM, et al. Bone and metal: An orthopaedic perspective on osseointegration of metals. *Acta Biomater.* 2014;10(10):4043–4057.
- [7] Sharma B, Kumar S, Ameyama K. Microstructure and properties of beta Ti–Nb alloy prepared by powder metallurgy route using titanium hydride powder. *J Alloys Compd.* 2016;656:978–986.

- [8] Li Y, Yang C, Zhao H, et al. New developments of Ti-based alloys for biomedical applications. *Materials (Basel)*. 2014;7(3):1709–1800.
- [9] Fan A, Ma Y, Yang R, et al. Friction and wear behaviors of Mo-N modified Ti6Al4V alloy in Hanks' solution. *Surf Coatings Technol*. 2013;228:S419–S423.
- [10] Wilson JCA, Ban S, Housden J, et al. On the response of Ti–6Al–4V and Ti–6Al–7Nb alloys to a Nitron-100 treatment. *Surf Coat Technol*. 2014;260:335–346.
- [11] Ng KW, Man HC, Cheng FT, et al. Laser cladding of copper with molybdenum for wear resistance enhancement in electrical contacts. *Appl Surf Sci*. 2007;253(14):6236–6241.
- [12] Viteri D, Barandika G, Bayo R, et al. Development of Ti–C–N coatings with improved tribological behavior and antibacterial properties. *J Mech Behav Biomed Mater*. 2016;55:75–86.
- [13] Tsipas SA, Gordo E, Jiménez-Morales A. Oxidation and corrosion protection by halide treatment of powder metallurgy Ti and Ti6Al4V alloy. *Corros Sci*. 2014;88:263–274.
- [14] Almeida A, Gupta D, Loable C, et al. Laser-assisted synthesis of Ti-Mo alloys for biomedical applications. *Mater Sci Eng C*. 2012;32(5):1190–1195.
- [15] Mandracci P, Mussano F, Rivolo P, et al. Surface treatments and functional coatings for biocompatibility improvement and bacterial adhesion reduction in dental implantology. *Coatings*. 2016. 6(1):7.
- [16] Sullivan SJL, Topoleski LDT. Surface modifications for improved wear performance in artificial joints: a review. *Miner Met Mater Soc*. 2015;67(11):2502–2517.
- [17] Mohammed MT, Khan ZA, Siddiquee AN. Surface modifications of titanium materials for developing corrosion behavior in human body environment: a review. *Procedia Mater Sci*. 2014;6(Icmpc):1610–1618.
- [18] Bolzoni L, Esteban PG, Ruiz-Navas EM, et al. Mechanical behaviour of pressed and sintered titanium alloys obtained from master alloy addition powders. *J Mech Behav Biomed Mater*. 2012;15:33–45.
- [19] Carman A, Zhang LC, Ivasishin OM, et al. Role of alloying elements in microstructure evolution and alloying elements behaviour during sintering of a near- $\beta$  titanium alloy. *Mater Sci Eng A*. 2011;528(3):1686–1693.
- [20] Ureña J, Mendoza C, Ferrari B, et al. Surface modification of powder metallurgy titanium by colloidal techniques and diffusion processes for biomedical applications. *Adv Eng Mater*. 2017;19(6):1–8.
- [21] Tsipas SA, Gordo E. Molybdeno-aluminizing of powder metallurgy and wrought Ti and Ti-6Al-4V alloys by pack cementation process. *Mater Charact*. 2016;118:494–504.
- [22] Sidambe AT. Biocompatibility of advanced manufactured titanium implants – a review. *Materials (Basel)*. 2014;7:8168–8188.
- [23] Divinski S, Hisker F, Klinkenberg C, et al. Niobium and titanium diffusion in the high niobium-containing Ti-54Al-10Nb alloy. *Intermetallics*. 2006;14(7):792–799.
- [24] Cardoso FF, Ferrandini PL, Lopes ESN, et al. Ti-Mo alloys employed as biomaterials: effects of composition and aging heat treatment on microstructure and mechanical behavior. *J Mech Behav Biomed Mater*. 2014;32:31–38.
- [25] Mi-Kyung H, Jai-Youl K, Moon-Jin H, et al. Effect of Nb on the microstructure, mechanical properties, corrosion behavior, and cytotoxicity of Ti-Nb alloys. *Materials (Basel)*. 2015;8:5986–6003.
- [26] Peng XM, Xia CQ, Liu YY, et al. Surface molybdenizing on titanium by halide-activated pack cementation. *Surf Coatings Technol*. 2009;203(20–21):3306–3311.
- [27] Li J, Xia C, Gu Y. Effect of temperature on microstructure of molybdenum diffusion coating on titanium substrate. *J Cent South Univ Technol*. 2004;11(1):15–18.
- [28] Gong J, Wu J, Guan Z. Examination of the indentation size effect in low-load Vickers hardness testing of ceramics. *J Eur Ceram Soc*. 1999;19:2625–2631.
- [29] Nnamchi PS, Njoku RE, Fasuba OA. Alloy design and property evaluation of Ti-Mo-Nb-Sn alloy for biomedical applications. *Niger J Technol*. 2013;32(3):410–416.
- [30] Oliveira NTC, Guastaldi AC. Electrochemical stability and corrosion resistance of Ti-Mo alloys for biomedical applications. *Acta Biomater*. 2009;5(1):399–405.
- [31] Matkovic P. Alloy design and property evaluation of new Ti–Cr–Nb alloys. *Mater Des*. 2012;33:26–30.
- [32] Neacsu P, Gordin D, Mitran V, et al. In vitro performance assessment of new beta Ti–Mo–Nb alloy compositions. *Mater Sci Eng C*. 2015;47:105–113.
- [33] Calderon-Moreno JM, Vasilescu C, Drob SI, et al. Microstructural and mechanical properties, surface and electrochemical characterisation of a new Ti-Zr-Nb alloy for implant applications. *J Alloys Compd*. 2014;612:398–410.
- [34] Mendes MWD, Ágrede CG, Bressiani AHA, et al. A new titanium based alloy Ti-27Nb-13Zr produced by powder metallurgy with biomimetic coating for use as a biomaterial. *Mater Sci Eng C*. 2016;63:671–677.